E3-2022-43

A. M. Sukhovoj, L. V. Mitsyna

A POSSIBILITY OF SIMULTANEOUS OBTAINING OF THE NUCLEAR LEVEL DENSITY AND RADIATIVE STRENGTH FUNCTIONS WHEN ANALYZING $(n, 2\gamma)$ REACTION

Суховой А. М., Мицына Л. В. E3-2022-43

Возможность одновременного получения ядерной плотности уровней и радиационных силовых функций при анализе $(n, 2\gamma)$-реакции

Для 43 компаунд-ядер массового диапазона $40 \leqslant A \leqslant 200$ накоплены наиболее вероятные ядерно-физические параметры (радиационные силовые функции и плотность ядерных уровней), полученные эмпирическим методом анализа высокоточных экспериментальных интенсивностей двухквантового каскадного γ-распада ядра после захвата теплового нейтрона. Метод позволяет определять сильно коррелирующие ядерно-физические параметры из непрямого эксперимента одновременно, что способствует изучению внутриядерных процессов. Приведены результаты эмпирического анализа для всех исследованных ядер при тестировании вариантов модельных представлений энергетических зависимостей искомых ядерно-физических параметров.

Работа выполнена в Лаборатории нейтронной физики им. И. М. Франка ОИЯИ.

Сообщение Объединенного института ядерных исследований. Дубна, 2022

Sukhovoj A. M., Mitsyna L. V. E3-2022-43

A Possibility of Simultaneous Obtaining of the Nuclear Level Density and Radiative Strength Functions When Analyzing $(n, 2\gamma)$ Reaction

For 43 compound nuclei from the $40 \leqslant A \leqslant 200$ mass region, the most probable nuclear-physical parameters (the radiative strength functions and nuclear level density) were accumulated obtained by the empirical method of analysis of precise experimental intensities of the two-step γ cascades in nucleus decaying after thermal neutron capture. The method allows obtaining the strongly correlated nuclear-physical parameters from indirect experiment simultaneously which enables to investigate the intranuclear processes. The results of the empirical analysis are presented for all investigated nuclei when testing versions of model representations of energy dependences of the required nuclear-physical parameters.

The investigation has been performed at the Frank Laboratory of Neutron Physics, JINR.

Communication of the Joint Institute for Nuclear Research. Dubna, 2022

INTRODUCTION

A study of the γ decay of an excited nucleus to obtain the nuclear level density and radiative strength functions is very important both for prediction of expected spectra of gammas in any nucleus and for calculation of neutron cross sections. The main purpose of such investigations at the low energies of nuclear excitation is the obtaining of noncontradictory representation of nuclear properties. As a modern theory supposes that the wave function of any excited level includes both quasi-particle and phonon components, simultaneous obtaining of the strongly correlated nuclear-physical parameters (nuclear level density ρ and partial widths Γ of a reaction-product emission) is needed not only for practical application, but also for investigation of fundamental intranuclear processes.

Analysis of data of indirect experiment in order to obtain the strongly correlated parameters ρ and Γ always leads to inevitability of unknown sizeable systematical errors. When γ-quanta coincidences are being recorded, indeterminateness of the nuclear-physical parameters obtained from the measured intensities of the two-step cascades is diminished in the presence of information about initial, final and intermediate cascade levels. But, with all this going on, there is a need to use the model representations of $\rho(E_{\rm ex})$ and $\Gamma(E_\gamma)$ functions, where $E_{\rm ex}$ and E_γ are energies of nuclear excitation and of γ quantum, because there is no possibility to determine experimentally the excitation energies and lifetimes of all intermediate levels of the cascades, as well as multipolarity of all γ transitions. The used models had to provide an accuracy of calculation, which conforms to description of the experimental spectra within their uncertainties.

As a rule, when describing the experimental γ spectrum, for the representation of the nuclear level density, $\rho(E_{\rm ex})$, the models from the Reference Input Parameter Library (RIPL) [1] (Gilbert–Cameron approach, back-shifted Fermi gas model, generalized superfluid model) are used. Because of simplicity of the above-mentioned models, they are recommended for calculating the level density for all nuclei from valley of stability. And available models for the radiative strength functions, $k(E_\gamma)$, are suitable for using in the excitation-energy region to the neutron binding energy. But there are problems connected with inexactness of these available models — the experimental spectra of the γ decay are not described with adequate accuracy. A modern theory of a nucleus furthers more realistic microscopic calculations of the nuclear level density taking into account pairing interactions of nucleons in nuclei, existence of collective levels in them, as well as nuclear-shell and

The values used in the empirical analysis

Nucleus	E_d, MeV	$E_{\max}$, MeV	Shell correction δE, MeV	I, %	Spins of λ state	Key No.
^{40}K	2.985	1.64	–3.1	67(3)	1, 2	2002VA28, 1987BO53
^{52}V	0.846	0.147	–5.0	60(2)	3, 4	2014LU01
^{60}Co	1.515	1.5	–5.9	71(3)	3, 4	2003SU36, 2005SU21
^{64}Cu	0.926	0.278	–3.2	30(6)	1, 2	2014KLU02
^{71}Ge	1.298	0	–3.5	32(2)	1/2	2004HO25
^{74}Ge	2.963	2.165	–3.0	36(2)	4, 5	2004HO25
^{114}Cd	2.316	0.558	–1.0	26(1)	0, 1	2005SU28, 1996VA25
^{118}Sn	2.930	1.230	–1.8	31(1)	0, 1	2006HO23, 2004GU12
^{124}Te	2.702	0.603	–0.3	20(2)	0, 1	1994VA44, 1995GE06
^{125}Te	1.319	0.671	–2.3	31(1)	1/2	1997KHZY, 2006BOZU
^{128}I	0.434	0.434	–1.0	33(2)	2, 3	1997AL29
^{137}Ba	2.662	0.279	–6.3	59(4)	1/2	1995BO57, 1995BO03
^{138}Ba	2.780	1.436	–8.2	26(5)	1, 2	1991BO55, 1993BO27
^{139}Ba	1.748	1.082	–6.0	81(6)	1/2	1991BO47, 1991BO57
^{140}La	0.658	0.322	–4.0	48(2)	3, 4	2000VA13, 2000VA30
^{150}Sm	1.927	0.773	3.0	12(1)	3, 4	1993VA15, 1995BO20
^{156}Gd	1.638	0.288	2.4	23(5)	1, 2	1993VA16, 1993KL03
^{158}Gd	1.517	0.261	–0.2	19(2)	1, 2	1994AL41
^{160}Tb	0.279	0.279	0.12	23(3)	1, 2	1999BO14, 1995VA42
^{163}Dy	1.055	0.250	–3.0	22(1)	1/2	1986BO43, 1988BO19
^{164}Dy	1.808	0.242	–2.0	29(1)	2, 3	1993VA17
^{165}Dy	0.738	0.184	–3.6	53(1)	1/2	1984PO18, 1984PO21
^{166}Ho	0.522	0.522	–1.5	31(1)	3, 4	2000PR10
^{168}Er	1.719	0.995	–2.3	27(4)	3, 4	2000SU21, 2000GR34
^{170}Tm	0.715	0.648	–1.3	23(2)	0, 1	1996VA23
^{172}Yb	1.849	0.260	–3.7	19(3)	0, 1	2017NG01
^{174}Yb	1.949	0.253	–3.5	22(1)	2, 3	1989BO53, 2008SU20
^{176}Lu	0.688	0.595	–1.8	44(1)	3, 4	1998KH14
^{177}Lu	0.854	0.637	0.25	16(1)	13/2, 15/2	1998KH05, 1993BE39
^{181}Hf	1.154	0.332	–3.1	52(4)	1/2	1991BO56, 1993VA14
^{182}Ta	0.480	0.360	–2.4	19(1)	3, 4	1997AL28
^{183}W	1.471	0.209	–4.0	28(1)	1/2	2005SU29, 1989BO30
^{184}W	1.431	0.364	–2.4	35(1)	0, 1	2002BOZV, 2003BO52
^{185}W	1.106	1.068	–0.9	62(1)	1/2	2002BO67
^{187}W	1.083	0.303	–2.6	34(1)	1/2	2005SU21, 2008BO26
^{188}Os	1.764	0.633	–0.2	59(3)	0, 1	2000BO49
^{190}Os	1.682	0.756	–0.7	49(3)	1, 2	2000BO50
^{191}Os	0.815	0.815	–3.5	76(2)	1/2	2008SU06, 1999BOZR
^{192}Ir	0.415	0.415	–0.3	27(6)	1, 2	1995VA41
^{193}Os	1.288	0.889	–3.8	80(1)	1/2	2002BO66
^{196}Pt	1.998	0.688	–3.7	37(5)	0, 1	1994AL50
^{198}Au	0.528	0.495	–5.6	42(1)	1, 2	1996MA75, 1995BO41
^{200}Hg	1.972	0.368	–8.0	59(2)	0, 1	1996VA24

deformation effects. But all model calculations must be tested on the base of reliable experimental data, which will also verify the reliability of the obtained nuclear-physical parameters.

In this paper, the results of the empirical analysis of the reaction of the radiative capture of the thermal neutrons are summarized for 43 nuclei from the $40 \leqslant A \leqslant 200$ mass region. The empirical method allowed obtaining simultaneously the most probable strongly correlated level densities and radiative strength functions of the excited compound nuclei analyzing the experimental intensities of their two-step cascade decay. The details of the analysis of all investigated nuclei are possible to clarify from the papers (on the website www-nds.iaea.org), the references are in the rightmost column of the Table.

1. EXPERIMENTAL POSSIBILITIES FOR THE TWO-STEP γ-DECAY INVESTIGATION

In the investigations of the two-step γ-cascade intensities, $I_{\gamma\gamma}(E_\gamma)$, by a technique of quanta-coincidences recording (with numerical improvement of resolution [2]), the energies of initial, intermediate and final cascade levels, as well as probabilities of transitions between them, are determined with a high accuracy. Spin interval is determined by spins of captured states and the selection rules for dipole transitions. Purely quadrupole transitions in the investigated cascades were not observed.

An uncertainty in the quanta sequence exists even for the two-step cascades, but the presence of energy-resolved peaks in the experimental spectrum allows the use of available spectroscopic data [3] about known intense transitions. For a part of energy-resolved two-step γ cascades, the quanta sequence can be determined unambiguously. High purity germanium (HPGe) detectors, which are used to record the quanta coincidences, collected the events of total capture of the cascade energy in narrow peaks (with full width at half maximum $\approx 7{-}8$ keV near the neutron binding energy B_n). Even in deformed nuclei, more than a half of measured intensity was composed of energy-resolved peaks.

The accuracy of the experimental $I_{\gamma\gamma}(E_1)$-spectrum shape, where E_1 is the energy of primary γ quantum of the cascade, was quite enough for the further analysis. The intensity spectra were normalized on the detection efficiency keeping a total number of recorded events.

2. PROCEDURE OF EXPERIMENTAL DATA ANALYSIS

The part of intensity of primary transitions, $I_{\gamma\gamma}(E_1)$, of the total experimental intensity, $I_{\gamma\gamma}(E_\gamma)$, of the two-step cascades in any small energy interval ΔE_j may be presented by the equation

$$I_{\gamma\gamma}(E_1) = \sum_{\lambda,f} \sum_i \frac{\Gamma_{\lambda i}}{\Gamma_\lambda} \frac{\Gamma_{if}}{\Gamma_i} = \sum_{\lambda,f} \sum_j \frac{\Gamma_{\lambda j}}{\langle \Gamma_{\lambda j} \rangle M_{\lambda j}} n_j \frac{\Gamma_{jf}}{\langle \Gamma_{jf} \rangle m_{jf}}. \qquad (1)$$

In each interval ΔE_j, there are n_j intermediate levels i of all types, and $M_{\lambda j}$ primary transitions from compound state λ fall to them, following which m_{jf} secondary transitions from them fall to final levels f (in a given energy interval, $n_j = \rho \Delta E_j$ and $m_{jf} = \rho \Delta E_j$, and ρ is a constant level density). As $\langle \Gamma_{\lambda j} \rangle = \Sigma_j \Gamma_{\lambda j} / M_{\lambda j}$ and $\langle \Gamma_{jf} \rangle = \Sigma_j \Gamma_{jf} / m_{jf}$, so sums of partial widths $\Sigma_j \Gamma_{\lambda j}$ of primary transitions and $\Sigma_j \Gamma_{jf}$ of secondary transitions can be written as $\langle \Gamma_{\lambda j} \rangle M_{\lambda j}$ and $\langle \Gamma_{jf} \rangle m_{jf}$, correspondingly.

The model representations of energy dependences, $\rho(E_{\text{ex}})$ and $k(E_1) = \Gamma / (A^{2/3} \cdot E_1^3 \cdot D_\lambda)$, where D_λ is an average distance between nuclear levels, are indispensable in the analysis, and for given functions $\rho(E_{\text{ex}}) = \varphi(p_1, p_2, \ldots)$ and $k(E_1) = \psi(q_1, q_2, \ldots)$, which are parameterized by fitted parameters p and q, the system of equations (1) has only one solution. It is important that the model representations of the nuclear-physical parameters are tested and modified in the course of the analysis, which leads to the best experimental spectra description.

Average amplitudes of changing of correction-vector components (usually less than 1% of current values of the set of fitted parameters) decrease at each iteration resulting in χ^2 minimum:

$$\chi^2 = \sum_{n_j} \frac{(I_{\gamma\gamma}^{\text{cal}}(E_1) - I_{\gamma\gamma}^{\text{exp}}(E_1))^2}{\sigma^2}, \qquad (2)$$

where $I_{\gamma\gamma}^{\text{cal}}(E_1)$ and $I_{\gamma\gamma}^{\text{exp}}(E_1)$ are model-parameterized and experimental intensities, and σ^2 is a dispersion of their difference. And there is no need to use any hypothesis untested experimentally.

3. MODEL REPRESENTATIONS OF THE NUCLEAR-PHYSICAL PARAMETERS

As the uncertainties of the obtained $\rho(E_{\text{ex}})$ and $k(E_1)$ functions are mainly determined by inexactness of their model-phenomenological functions, $\varphi(p_1, p_2, \ldots)$ and $\psi(q_1, q_2, \ldots)$, so the most probable nuclear level density and radiative strength functions can be determined only by a comparison of the best $I_{\gamma\gamma}(E_1)$ fittings with different model representations of required $\rho(E_{\text{ex}})$ and $k(E_1)$ functions and with wide intervals of variation of fitted parameters, $p_1, p_2, \ldots$ and $q_1, q_2, \ldots$

The used in the analysis model-phenomenological energy dependences of the required nuclear-physical parameters were parameterized on the base of their existing representations to have a potential possibility of their smoothness breaking. A convincing argument of such a modification appeared at the first steps of using the empirical analysis of $I_{\gamma\gamma}(E_\gamma)$ intensity [4], when the fitted parameters were deformed in a random way by small deviations (by Gaussian curves with different dispersions and averages) without using any model representations of the required functions. At a slow convergence of the process of χ^2 minimization, the breaks have been observed in the $\rho(E_{\text{ex}})$ functions of heavy nuclei for the first time. Taking this fact into account in

parameterization of $\varphi(p_1, p_2, \ldots)$ and $\psi(q_1, q_2, \ldots)$ functions greatly accelerates the fittings.

3.1. Models of the Nuclear Level Density. A description of the intensities of the two-step cascades in a nucleus below B_n showed inexactitude of predictions of the Fermi gas model [5], as well as postulated smoothness of the phenomenological coefficient of the collective enhancement of the level density [6]. Taking into account a possibility of an existence of breaks in the model $\rho(E_{\rm ex})$ functions, an expression for the density of levels ρ_l of fermion type was parameterized on the base of the model of density Ω_n of n-quasi-particle nuclear excitations [7], which is successfully applied to describe the spectra of pre-equilibrium reactions

$$\rho_l = \frac{(2J+1)\cdot \exp\left(-(J+1/2)^2/2\sigma^2\right)}{2\sqrt{2\pi}\,\sigma^3}\ \Omega_n(E_{\rm ex}),$$
$$\Omega_n\left(E_{\rm ex}\right) = \frac{g^n(E_{\rm ex}-U_l)^{n-1}}{((n/2)!)^2(n-1)!}. \qquad (3)$$

Here, cut-off factor σ of the spin J for the excited state of compound nucleus above the maximal excitation energy E_d of a discrete-level area and a density $g = 6a/\pi^2$ of singe-particle states near the Fermi surface are taken from the model [5], and U_l is an energy of the lth break in the $\rho(E_{\rm ex})$ energy dependence (the likely breaking threshold of the lth Cooper pair of nucleons in a nucleus).

An influence of the shell correction δE on the density of the quasi-particle levels was also tested by inclusion of δE values calculated for 43 investigated nuclei (see the 4th column of the Table) to some model-parameterization variants of the $\rho(E_{\rm ex})$ function. The shell inhomogeneities of a single-particle spectrum were taken into account by means of inclusion of the correction to excitation-energy dependence of a value, which linearly enters into the coefficient $g = 6a/\pi$ from Eq. (3):

$$a(A, E_{\rm ex}) = \widetilde{a}(1 + ((1 - \exp\left(\gamma E_{\rm ex}\right))\,\delta E/E_{\rm ex})). \qquad (4)$$

An asymptotic value $\widetilde{a} = 0.114A + 0.162A^{2/3}$ and coefficient $\gamma = 0.054$ were taken from [6]. The shell values δE calculated from the data of mass defect in a liquid-drop nuclear model from [6] were lightly corrected in order to keep an average distance D_λ between resonances of investigated nuclei.

The commonly accepted phenomenological coefficient $C_{\rm col}$ of the collective enhancement of the vibrational level density (or both vibrational and rotational ones for deformed nuclei) [6], taking into account a possibility of sequential breaks, is written as

$$C_{\rm col} = A_l \exp\left(\sqrt{(E_{\rm ex}-U_l)/E_u} - (E_{\rm ex}-U_l)/E_u\right), \qquad (5)$$

where A_l are parameters of density of vibrational levels above each lth break, and parameter E_u determines a rate of a change in densities of quasi-particle and phonon levels. The analysis of the two-step γ-cascade intensities in all

investigated nuclei (see, for example, [8–10]) has demonstrated that, in the majority of them, E_u is practically equal to the average pairing energy Δ_0 of the last nucleon [11].

3.2. Models of the Dipole Radiative Strength Functions. Now all analytical representations of the radiative strength function are modifications of the model from [12] in which the influence of the tail of giant electrical dipole resonance on the Fermi liquid, as well as of phonon excitations at low energies, is taken into account. In the framework of the empirical method, it is possible to obtain not only the total strength function, $k(E_1) = k(E1, E_1) + + k(M1, E_1)$, but also its components for electrical and magnet transitions of the cascades, $k(E1, E_1)$ and $k(M1, E_1)$, separately.

The smooth part of the radiative strength functions (as in [12]) supplemented with additional fitted parameters of weight, w, and of a change of derivatives, κ, is written as

$$k(E_1) = w\frac{\Gamma_G^2(E_1^2 + \kappa 4\pi^2 T^2)}{(E_1^2 - E_G^2)^2 + E_G^2\,\Gamma_G^2}, \tag{6}$$

where E_G and Γ_G are location and width of the maximum of the giant dipole resonance [13], T is a varied nuclear thermodynamic temperature.

Taking into account that the required functions, $\rho(E_{\rm ex})$, $k(E1, E_1)$, and $k(M1, E_1)$, describe the γ-decay process in combination, a possibility of irregularities was included into the initial shape of the strength function distributions. Probability of an appearance of one–two peaks in the smooth strength functions (6) was provided by a supplement of additional fitted parameters to the $k(E_1)$ initial shape. A necessity of taking into account an asymmetry of peaks added to the $k(E_1)$ functions results from the theoretical analysis of the fragmentation of single-particle states at varied locations relative to the Fermi surface [14]. In different model variants, each local peak was described either by two exponents or by an asymmetrical Lorentzian curve.

In the first case, each local peak added to the smooth part (6) is expressed as

$$+P\delta^- \exp\left(\alpha_p(E_1 - E_p)\right) + P\delta^+ \exp\left(\beta_p(E_p - E_1)\right). \tag{7}$$

The first summand of Eq. (7) is the left skewing of the local peak (energies below its maximum), and the second summand is the right skewing of the peak (energies above maximum). For each local peak, its position, E_p, amplitude, P, left skewing parameter, α_p, and right skewing parameter, β_p, are fitted independently.

In the latter case, the additional peak item is written as

$$+\sum_i W_i\,\frac{(E_1^2 + (\alpha_i(E_i - E_1)/E_1))\Gamma_i^2}{(E_1^2 - E_i^2)^2 + E_1^2\Gamma_i^2}, \tag{8}$$

Here, parameters of each ith peak ($i \leqslant 2$) are a center position of the peak E_i, a peak width Γ_i, its amplitude W_i, and an asymmetry parameter $\alpha_i \sim T^2$.

The initial shapes of $k(E1, E_1)$ and $k(M1, E_1)$ distributions are written similarly, but all the parameters of both components of the strength function, which were mentioned in Eqs. (6)–(8), are fitted independently, and in the process of the χ^2 minimization at the $I_{\gamma\gamma}(E_1)$-intensity fitting, the initially similar shapes of $k(E1, E_1)$ and $k(M1, E_1)$ distributions are grossly changed.

At $E_1 \approx B_n$, the fitted ratios Γ_{M1}/Γ_{E1} of $E1$ and $M1$ transitions are normalized to known experimental values, and their sums Γ_λ — to the total radiative widths of the resonances.

4. RESULTS

For a majority of investigated nuclei, the number of fitted model parameters at a description of the experimental $I_{\gamma\gamma}(E_1)$ intensities is no more than 21. It is not too much for the energy-resolved cascades measured in cannels of $\approx$ 1-keV width. Furthermore, for the investigated nuclei, more than one energy-resolved cascade (up to 16 cascades in some of them) was observed. The required $\rho(E_{\rm ex}) = \varphi(U_l, E_u, A_l)$ and $k(E_1) = \psi(w, \kappa, E, \Gamma, \ldots)$ functions were calculated using their parameters fitted in describing the experimental $I_{\gamma\gamma}(E_1)$ spectra, which were averaged over $\Delta E_1 = 50$ keV. Such averaging turned out to be an optimal compromise between very detailed experimental spectrum and a search for general regularities of the γ-decay process. In Figs. 1 and 2, the experimental $I_{\gamma\gamma}(E_1)$ intensities, as well as their descriptions, are presented with larger ΔE_1 intervals, which are multiplied by ten, in order to show up the distinctive features of the decay process. Only one most precise of $I_{\gamma\gamma}(E_1)$ distributions measured studying $^{171}{\rm Yb}(n, 2\gamma)$ reaction [15] was shown averaged over $\Delta E_1 = 0.25$ MeV intervals.

For all investigated nuclei, in the Table, some values used in the analysis are presented: the maximal excitation (upper-bound) energies E_d of discrete-level areas, the upper excited final level of analyzed cascades $E_{\rm max}$, corrections δE on shell inhomogeneities of a single-particle spectrum, the part of the intensities $I(\%)$ of the two-step γ cascades in percent per one decay of compound states, and the spins of the decayed compound states.

The experimental data for 43 nuclei were analyzed with the use of four pairs of model modifications of the $\rho(E_{\rm ex})$ and $k(E_1)$ functions. In two variants of combinations of nuclear parameter models, shell inhomogeneities of the single-particle spectrum were taken into account (Eq. (4)), and in two others, $g = {\rm const}$ (Eq. (3)). In three of these variants, the exponential shapes of the local peaks (Eq. (7)) were taken in addition to the model representation of the radiative strength functions, and in the fourth variant, the local peaks were described by Lorentzian curves (Eq. (8)). The model variants also differed in a number of fitted parameters optimizing in the course of model testing for the best description of the experimental data.

In Figs. 1 and 2, histograms are the averaged experimental $I_{\gamma\gamma}(E_1)$ distributions with their uncertainties in percent per a compound-nucleus decay, and closed points are the best $I_{\gamma\gamma}(E_1)$ fits. Triangles in these figures

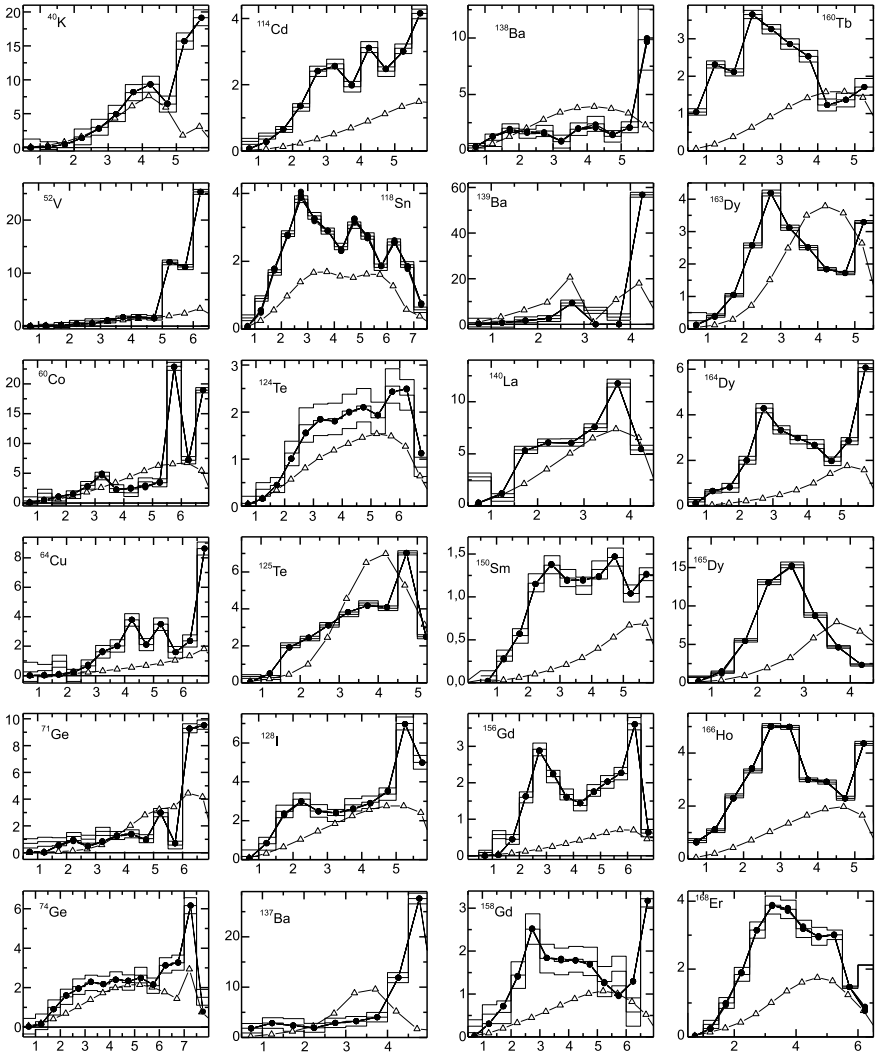

Fig. 1. The dependences of $I_{\gamma\gamma}(E_1)$ intensities (Y-axis, in percent per a compound-nucleus decay) on the energy of primary transitions (X-axis, in MeV) of the cascades in odd–odd ^{40}K, ^{52}V, ^{60}Co, ^{64}Cu, ^{128}I, ^{140}La, ^{160}Tb, ^{166}Ho, even–odd ^{71}Ge, ^{125}Te, ^{137,139}Ba, ^{163,165}Dy, and even–even ^{74}Ge, ^{114}Cd, ^{118}Sn, ^{124}Te, ^{138}Ba, ^{150}Sm, ^{156,158}Gd, ^{164}Dy, ^{168}Er nuclei: histograms are the averaged experimental $I_{\gamma\gamma}(E_1)$ intensities and their uncertainties; closed points are the best $I_{\gamma\gamma}(E_1)$ fits; triangles are calculated $I_{\gamma\gamma}(E_1)$ intensities using the statistical model from [5] and the model of [12] with $k(M1, E_1) = \text{const}$

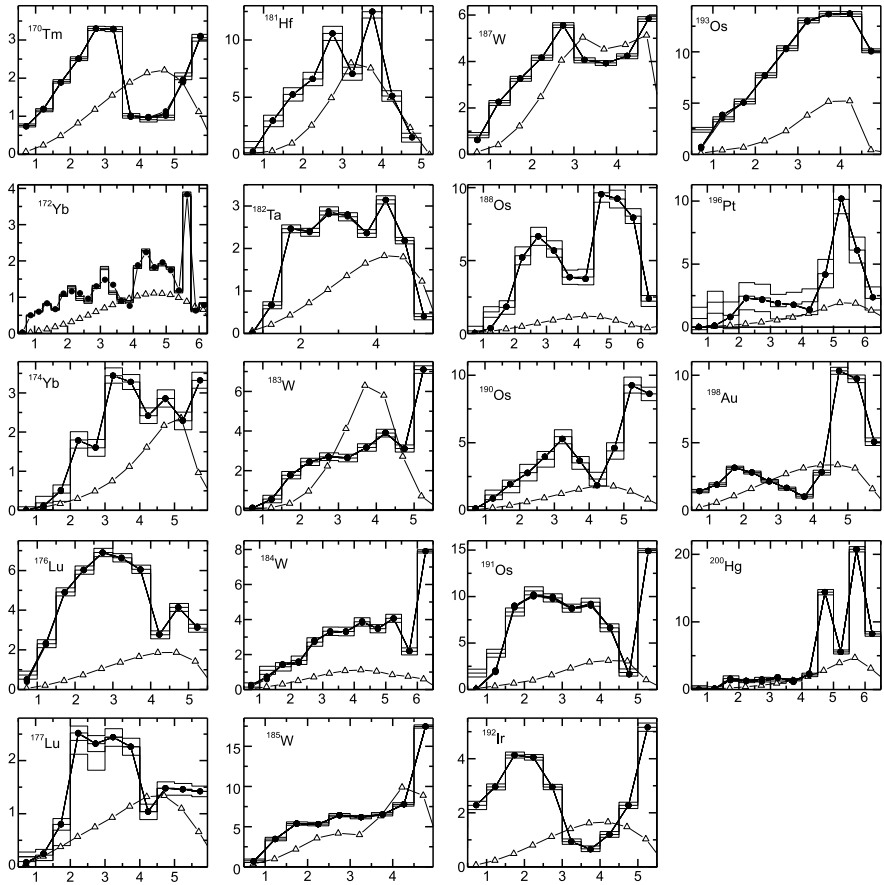

Fig. 2. The dependences of $I_{\gamma\gamma}(E_1)$ intensities (Y-axis, in percent per a decay) on the energy of primary transitions (X-axis, in MeV) of the cascades in odd–odd ^{170}Tm, ^{176}Lu, ^{182}Ta, ^{192}Ir, ^{198}Au, even–odd ^{181}Hf, ^{183,185,187}W, ^{191,193}Os, even–even ^{172,174}Yb, ^{184}W, ^{188,190}Os, ^{196}Pt, ^{200}Hg nuclei, and odd–even ^{177}Lu nucleus: histograms are the averaged experimental $I_{\gamma\gamma}(E_1)$ intensities and their uncertainties; closed points are the best $I_{\gamma\gamma}(E_1)$ fits; triangles are calculated $I_{\gamma\gamma}(E_1)$ intensities using the statistical model from [5] and the model of [12] with $k(M1, E_1) = \text{const}$

represent calculated $I_{\gamma\gamma}(E_1)$ intensities when the $\rho(E_{\text{ex}})$ function corresponds to prediction of the back-shifted Fermi gas model [5].

It was found that the data obtained for each of investigated 43 nuclei are individual. This fact corresponds to modern representations of dynamics of a nuclear-state fragmentation (the wave functions of excited nuclear levels are formed in a process of fragmentation of the states with different quantum numbers and varied locations relative to the Fermi surface) [14].

The given procedure of the experimental data analysis revealed an existence of breaks in the excitation-energy dependences of the nuclear level densities of all investigated nuclei. In Figs. 3 and 4, there are the $\rho(E_{\rm ex})$ distributions calculated using their parameters defined from the best $I_{\gamma\gamma}(E_1)$ fits. It turns out that the observed breaks in the $\rho(E_{\rm ex})$ energy dependences

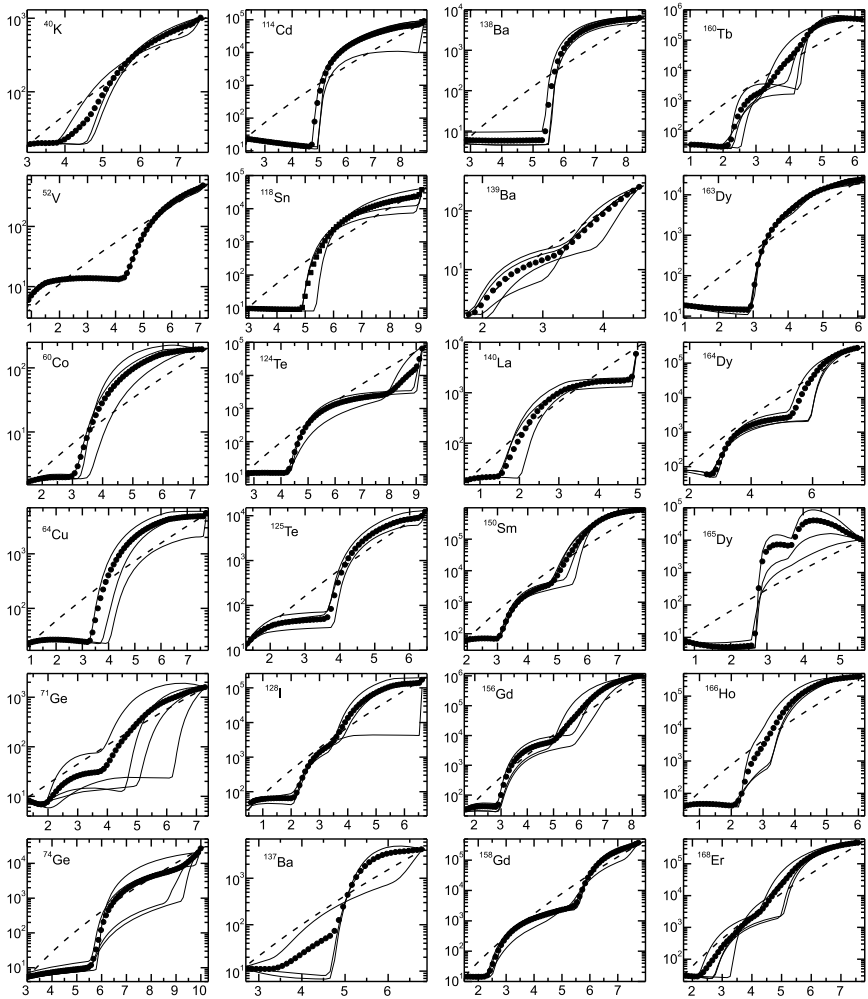

Fig. 3. The dependences of the level density $\rho(E_{\rm ex})$ (Y-axis, in MeV^{-1}) on the excitation energy (X-axis, in MeV) in odd–odd ^{40}K, ^{52}V, ^{60}Co, ^{64}Cu, ^{128}I, ^{140}La, ^{160}Tb, ^{166}Ho, even–odd ^{71}Ge, ^{125}Te, ^{137,139}Ba, ^{163,165}Dy, and even–even ^{74}Ge, ^{114}Cd, ^{118}Sn, ^{124}Te, ^{138}Ba, ^{150}Sm, ^{156,158}Gd, ^{164}Dy, ^{168}Er nuclei. In each picture: solid lines and closed points are the best fits; dashed lines are calculations according to the back-shifted Fermi gas model [5]

are located at a distance $\approx 2\Delta_0$ from each other in the excitation-energy scale, where Δ_0 is a paring energy of the last nucleons in a nucleus.

For a majority of investigated nuclei, the fact was established that determined energies of breaks, U_2 and U_3, which are possibly the breaking thresholds of the second and the third Cooper pairs of nuclear nucleons, weekly depend on excitation energy.

There is a principal evident distinction between the $\rho(E_{\rm ex})$ functions obtained analyzing γ decay in different nuclei. For example, three breaks have been observed in the excitation-energy distributions of the level density for

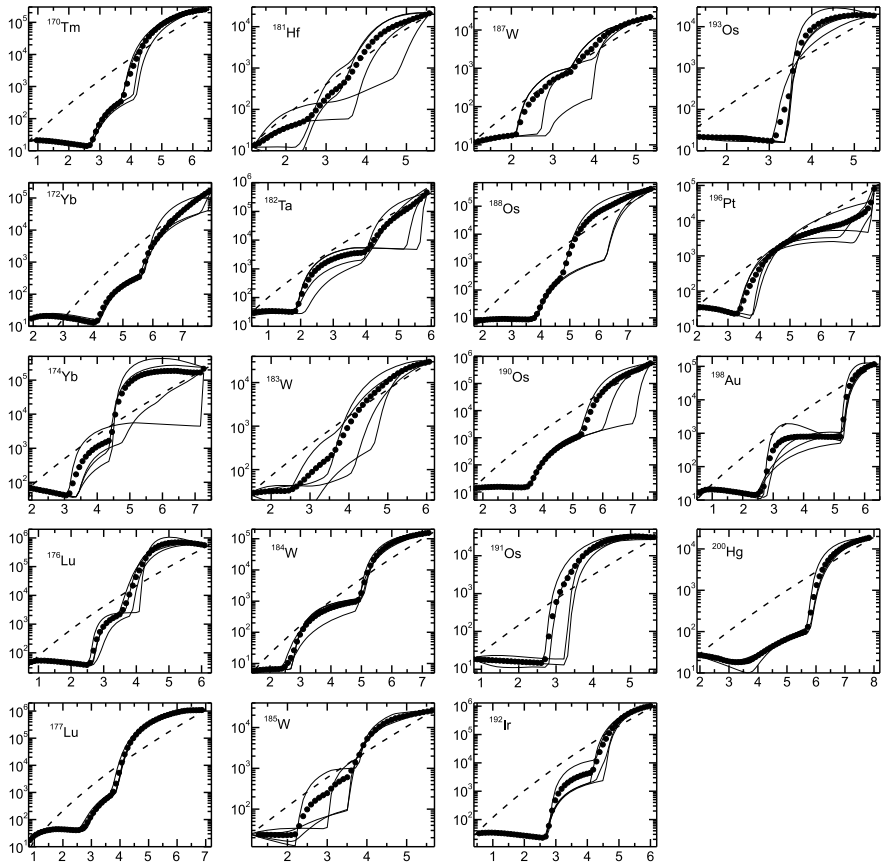

Fig. 4. The dependences of the level density $\rho(E_{\rm ex})$ (Y-axis, in MeV^{-1}) on the excitation energy (X-axis, in MeV) in odd–odd ^{170}Tm, ^{176}Lu, ^{182}Ta, ^{192}Ir, ^{198}Au, even–odd ^{181}Hf, ^{183,185,187}W, ^{191,193}Os, even–even ^{172,174}Yb, ^{184}W, ^{188,190}Os, ^{196}Pt, ^{200}Hg nuclei, and odd–even ^{177}Lu nucleus. In each picture: solid lines and closed points are the best fits; dashed lines are calculations according to the back-shifted Fermi gas model [5]

odd–odd ^{40}K, ^{52}V, ^{60}Co, ^{64}Cu, even–even ^{114}Cd, ^{118}Sn, ^{138}Ba, even–odd ^{137}Ba, ^{191,193}Os, and ^{163}Dy nuclei, while the number of breaks was greater by one in the $\rho(E_{\rm ex})$ functions of the rest of investigated nuclei. And almost all nuclei with three breaks in the $\rho(E_{\rm ex})$ functions, except for ^{163}Dy, are spherical ones.

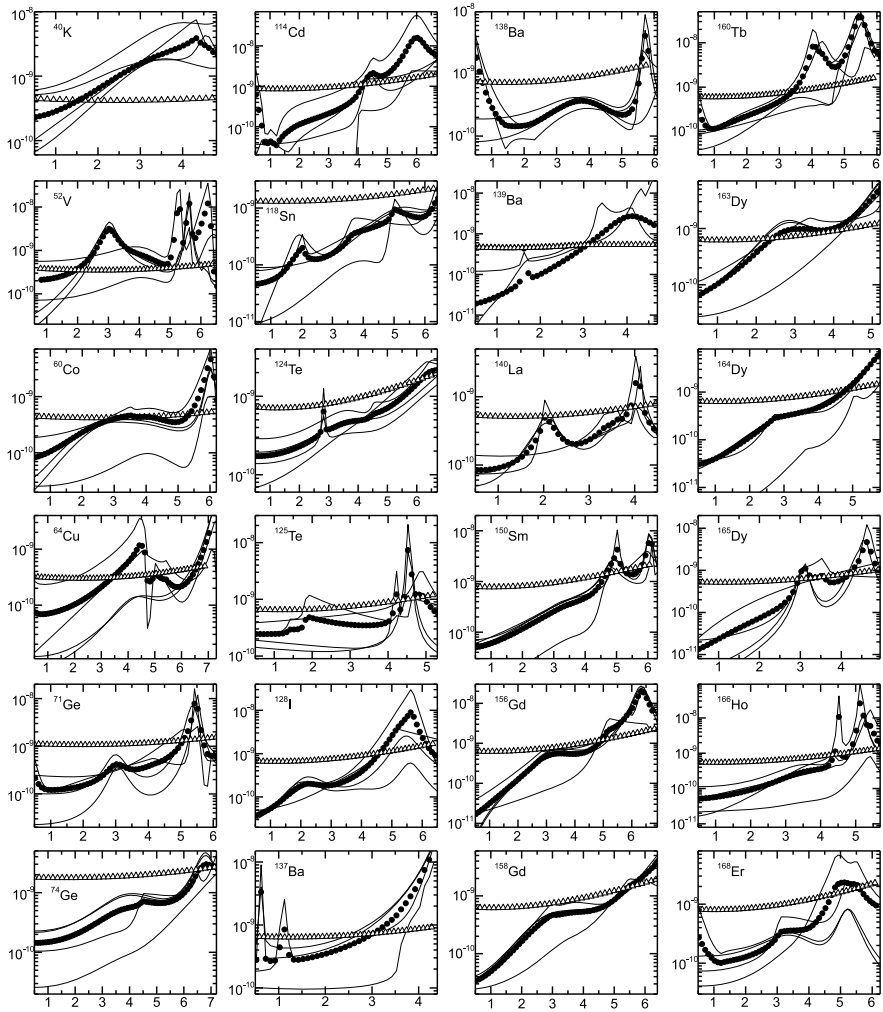

Fig. 5. The dependences of the sums, $k(E1,E_1)+k(M1,E_1)$, of the radiative strength functions (Y-axis, MeV^{-3}) on the energy of primary transitions (X-axis, MeV) of the cascades in odd–odd ^{40}K, ^{52}V, ^{60}Co, ^{64}Cu, ^{128}I, ^{140}La, ^{160}Tb, ^{166}Ho, even–odd ^{71}Ge, ^{125}Te, ^{137,139}Ba, ^{163,165}Dy, and even–even ^{74}Ge, ^{114}Cd, ^{118}Sn, ^{124}Te, ^{138}Ba, ^{150}Sm, ^{156,158}Gd, ^{164}Dy, ^{168}Er nuclei. In each picture: lines and closed points are the best fits; triangles are calculations according to the model of [12] with $k(M1,E_1)=$ const

As a rule, the derivatives of the $\rho(E_{\rm ex})$ functions obtained fitting the experimental intensities of the two-step cascades in all investigated nuclei are greater than the derivatives of these functions calculated using the predictions of the Fermi gas model (these calculations are presented in Figs. 3 and 4 by dashed lines). This effect can be associated with a sharp increase in the number of excited quasi-particles at small excitation energies. And an observed decline in a growth of $\rho(E_{\rm ex})$ derivatives near B_n energy is explained by the use in the empirical-method analysis of the phenomenological coefficient $C_{\rm col}$ (Eq. (5)), which predicts a decrease in the number of vibrational levels at these excitation energies.

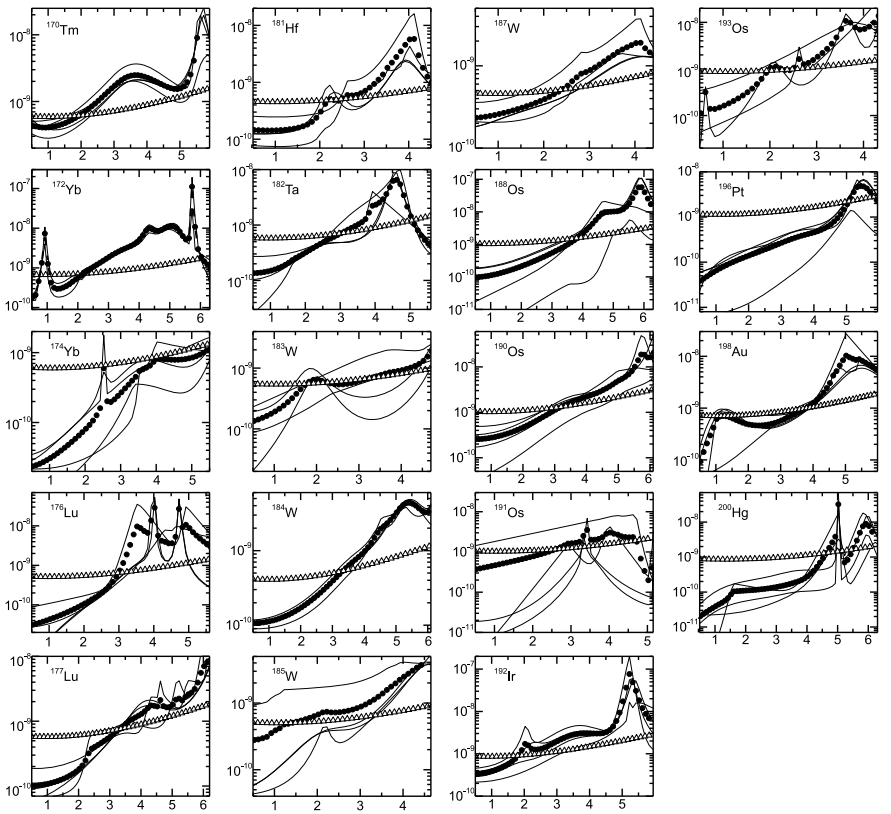

Fig. 6. The dependences of the sums, $k(E1,E_1)+k(M1,E_1)$, of the radiative strength functions (Y-axis, MeV^{-3}) on the energy of primary transitions (X-axis, MeV) of the cascades in odd–odd ^{170}Tm, ^{176}Lu, ^{182}Ta, ^{192}Ir, ^{198}Au, even–odd ^{181}Hf, ^{183,185,187}W, ^{191,193}Os, even–even ^{172,174}Yb, ^{184}W, ^{188,190}Os, ^{196}Pt, ^{200}Hg nuclei, and odd–even ^{177}Lu nucleus. In each picture: lines and closed points are the best fits; triangles are calculations according to the model of [12] with $k(M1,E_1)=\text{const}$

A comparison of the energy distributions of the nuclear level density obtained in the empirical analysis and calculated within the framework of the statistical back-shifted Fermi gas model (as well as by the Fermi gas model, taking into account shell inhomogeneities of single-particle spectrum) showed their obvious divergence.

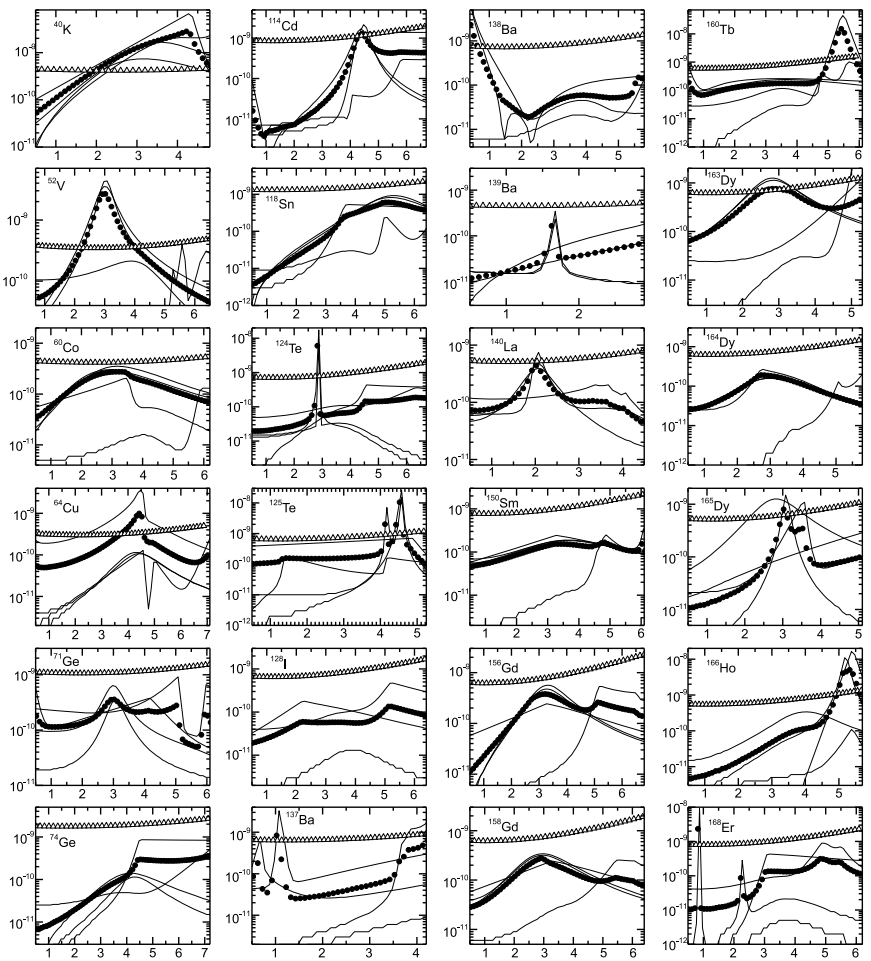

Fig. 7. The dependences of the radiative strength functions of magnet transitions $k(M1, E_1)$ (Y-axis, MeV^{-3}) on the energy of primary transitions (X-axis, MeV) of the cascades in odd–odd ^{40}K, ^{52}V, ^{60}Co, ^{64}Cu, ^{128}I, ^{140}La, ^{160}Tb, ^{166}Ho, even–odd ^{71}Ge, ^{125}Te, ^{137,139}Ba, ^{163,165}Dy, and even–even ^{74}Ge, ^{114}Cd, ^{118}Sn, ^{124}Te, ^{138}Ba, ^{150}Sm, ^{156,158}Gd, ^{164}Dy, ^{168}Er nuclei. In each picture: lines and closed points are the best fits; triangles are calculations of the radiative strength functions according to the model of [12] with $k(M1, E_1) = \text{const}$

All the investigated two-quanta cascades consist of only dipole γ transitions. In spite of anticorrelation between the radiative strength functions of $E1$ and $M1$ transitions, the empirical method allows obtaining both the energy dependence of their sum, $k(E1, E_1) + k(M1, E_1)$, and the functions, $k(E1, E_1)$ and $k(M1, E_1)$, separately.

It is seen from Figs. 5 and 6 that there is a characteristic feature of the radiative strength function — the sums, $k(E1, E_1) + k(M1, E_1)$, diminish twenty (or more) times over the whole investigated interval of nuclear excitation from 1 to 6 MeV. The $k(E_1)$ functions calculated with their fitted

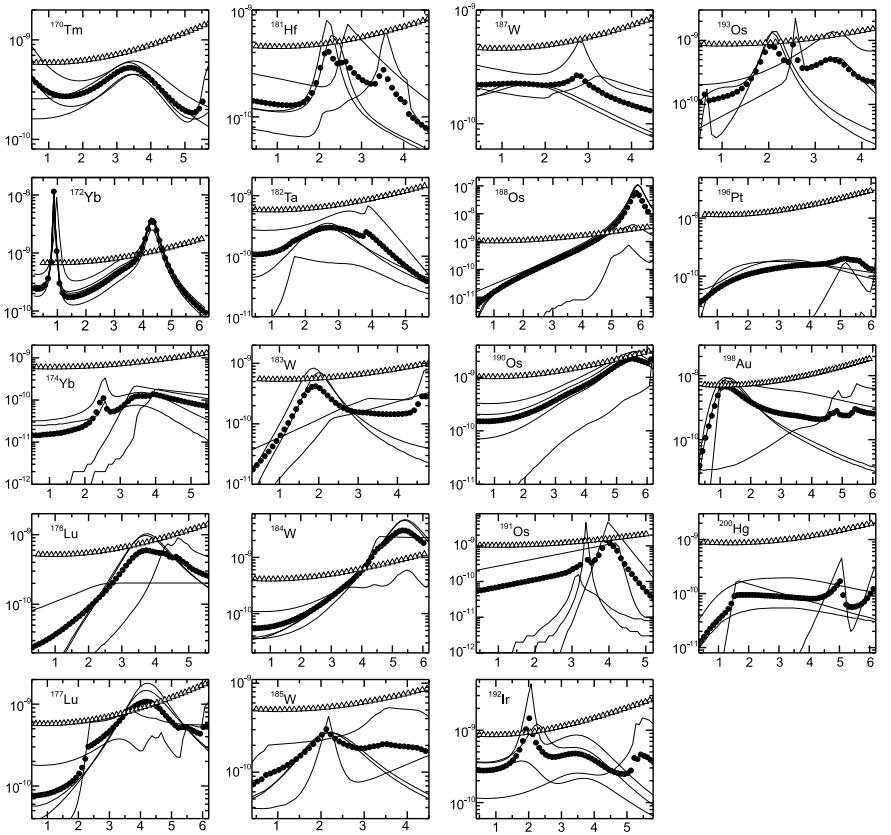

Fig. 8. The dependences of the radiative strength functions of magnet transitions $k(M1, E_1)$ (Y-axis, MeV^{-3}) on the energy of primary transitions (X-axis, MeV) of the cascades in odd–odd ^{170}Tm, ^{176}Lu, ^{182}Ta, ^{192}Ir, ^{198}Au, even–odd ^{181}Hf, ^{183,185,187}W, ^{191,193}Os, even–even ^{172,174}Yb, ^{184}W, ^{188,190}Os, ^{196}Pt, ^{200}Hg nuclei, and odd–even ^{177}Lu nucleus. In each picture: lines and closed points are the best fits; triangles are calculations of the radiative strength functions according to the model of [12] with $k(M1, E_1) = \text{const}$

parameters always cross the ones predicted by the model [12] (triangles in Figs. 5–8). The sums $k(E1, E_1) + k(M1, E_1)$ are, most probably, minimal for nuclei with opposite parities of the decayed compound state and final levels of the cascades.

In Figs. 7 and 8, the radiative strength functions of the magnet transitions in investigated nuclei are separately presented. For a majority of nuclei, a maximum of $k(M1, E_1)$ function is located below a maximum of $k(E1, E_1)$ function.

A scatter of data on $k(E_1)$ functions obtained from the $I_{\gamma\gamma}(E_1)$ approximations is noticeably wider than that on $\rho(E_{\rm ex})$ functions. An essential ambiguity of the radiative strength functions can be explained by different dependency of $k(E1, E_1)$ and $k(M1, E_1)$ functions on the intermediate-level density and impossibility to determine experimentally the parities of these intermediate levels (or, at least, to ascertain a part of levels with a certain parity) in the observable excitation-energy region of $E_d \leqslant E_{\rm ex} \leqslant B_n - 0.52$ MeV.

CONCLUSIONS

A possibility of simultaneous obtaining of the strongly correlated $\rho(E_{\rm ex})$ and $k(E_1)$ functions from indirect experiment is offered only by the Dubna empirical method, which allows a description of modern experiment $I_{\gamma\gamma}(E_\gamma)$ data with an accuracy within their experimental uncertainties.

Using four different variants of the experimentally tested model representations of the $\rho(E_{\rm ex})$, $k(E1, E_1)$, and $k(M1, E_1)$ energy dependences, these strongly correlated nuclear-physical parameters were obtained for 43 nuclei with the accuracy which is the most achievable by now.

The steps discovered in the energy dependences of the nuclear level density can be explained by a sequential breaking of nucleon pairs in an excited nucleus.

As there is no way to take into account all evident nonstatistical effects in the model representations of the nuclear parameters, from the practical standpoint, location within the strongly statistical framework does not allow one to clarify a picture of intranuclear interaction of boson and fermion nuclear states of nuclear matter.

For a higher reliability of the obtained nuclear level density and radiative strength functions, the modern models of an excited nucleus and its γ decay which includes the reaction products are demanded. All the models can be tested in the empirical method of the analysis.

Acknowledgements. The authors deeply appreciate an important contribution of Dr. V. Khitrov to the empirical analysis development and are grateful to Drs. N. Jovančević and D. Knežević from the University of Novi Sad, Serbia, and to Dr. Nguyen Ngoc Anh from the Dalat Nuclear Research Institute, Vietnam, for the helpful cooperation.

REFERENCES

1. Reference Input Parameter Library RIPL-2. Handbook for Calculations of Nuclear Reaction Data. IAEA-TECDOC, 2002.
2. *Boneva S. T., Sukhovoj A. M., Khitrov V. A., Voinov A. V.* Excitation Study of High-Lying States of Differently Shaped Heavy Nuclei by the Method of Two-Step Cascades // Nucl. Phys. 1995. V. 589. P. 293–306.
3. *Popov Yu. P., Sukhovoj A. M., Khitrov V. A., Yazvitsky Yu. S.* Study of the γ Decay of ^{165}Dy with the Help of the $(n, 2\gamma)$ Reaction // Bull. Acad. Sci. USSR Phys. Ser. 1984. V. 48, No. 5. P. 53.
4. *Vasilieva E. V., Sukhovoj A. M., Khitrov V. A.* Direct Experimental Estimate of Parameters That Determine the Cascade Gamma Decay of Compound States of Heavy Nuclei // Phys. At. Nucl. 2001. V. 64. P. 153–168.
5. *Dilg W., Schantl W., Vonach H., Uhl M.* Parameters for the Back-Shifted Fermi Gas Model in the Mass Range $40 < A < 250$ // Nucl. Phys. A. 1973. V. 217. P. 269–298.
6. *Ignatyuk A. V.* Statistical Properties of Excited Atomic Nuclei. Report INDC-233(L), IAEA, Vienna, 1985.
7. *Strutinsky V. M.* On the Nuclear Level Density in Case of an Energy Gap // Proc. of the Intern. Congress on Nuclear Physics, Paris, France, 1958. P. 617–622.
8. *Sukhovoj A. M.* New Model of the Cascade Gamma Decay of Neutron Resonances for Practitioners: Basic Concepts and Attainable Precision // Phys. At. Nucl. 2015. V. 78. P. 230–245.
9. *Sukhovoj A. M., Mitsyna L. V., Jovančević N.* Picture of the Cascade Gamma Decay of Neutron Resonances within a Modified Practical Model // Phys. At. Nucl. 2016. V. 79, No. 3. P. 313–325.
10. *Vu D. C., Sukhovoj A. M., Mitsyna L. V., Zeinalov Sh., Jovančević N., Kneževič D., Krmar M., Dragić A.* Representation of Radiative Strength Functions within a Practical Model of Cascade Gamma Decay // Phys. At. Nucl. 2017. V. 80, No. 2. P. 237–250.
11. *Kravtsov V. A.* Atomic Masses and Nuclear Binding Energies. Moscow: Atomizdat, 1965. 375 p. (in Russian).
12. *Kadmensky S. G., Markushev V. P., Furman W. I.* Radiative Widths of Neutron Resonances. Giant Dipole Resonances // Sov. J. Nucl. Phys. 1983. V. 37. P. 165.
13. *Mughabghab S. F., Divadeenam M., Holden N. E.* Neutron Cross Sections. Neutron Resonance Parameters and Thermal Cross Sections. National Nuclear Data Center, BNL, Acad. Press, 1981.
14. *Malov L. A., Soloviev V. G.* General Regularities of Fragmentation of Single-Particle States in Deformed Nuclei // Sov. J. Nucl. Phys. 1977. V. 26. P. 384.
15. *Nguyen N. A., Nguyen X. N., Pham D. K., Vu D. C., Sukhovoj A. M., Mitsyna L. V.* Thresholds for the Break of Nucleon Cooper Pairs and Special Features of the Decay of the ^{172}Yb Nucleus in the Reaction $^{171}\mathrm{Yb}(n_{\mathrm{th}}, 2\gamma)$ // Phys. At. Nucl. 2018. V. 81, No. 3. P. 296–306.

Received on October 17, 2022.

Редактор *В. В. Булатова*

Подписано в печать 23.11.2022.
Формат 60 × 90/16. Бумага офсетная. Печать офсетная.
Усл. печ. л. 1,25. Уч.-изд. л. 1,36. Тираж 115 экз. Заказ № 60541.

Издательский отдел Объединенного института ядерных исследований
141980, г. Дубна, Московская обл., ул. Жолио-Кюри, 6.
E-mail: publish@jinr.ru
www.jinr.ru/publish/